THE EFFECT OF NONLINEARITY AND FORCING ON GLOBAL MODES

J. M. Chomaz

Meteorologie Nationale CNRM
42 Avenue G Coriolis
31057 Toulouse Cedex, France

P. Huerre and L. G. Redekopp

Department of Aerospace Engineering
University of Southern California
Los Angeles, California, USA 90089-1191

1 REVIEW OF RELEVANT CONCEPTS

Representation of the linear disturbance field in terms of local modes is firmly established for wave guides where the propagation space is homogeneous. Local modes, although discretized in the transverse or wave-guide dimension(s), are continuous in the streamwise or propagation-space dimension(s) by virtue of the translational invariance of the system. Specifically, considering a two-space-dimension problem with x being a coordinate in the propagation direction and y being a transverse, wave-guide coordinate, an arbitrary disturbance field is expressible as the superposition of eigenmodes of the form $\phi(y)\exp\{i(kx - \omega t)\}$, where the complex frequency ω and wave number k are related through a dispersion relation

$$D(\omega, k; \mu) = 0. \tag{1.1}$$

The symbol μ is used to represent the control parameter(s) of the problem. The dispersion relation specifies such stability characteristics of the local modes as the temporal growth rate $\omega_i = Im\omega$, the spatial growth rate $-k_i = -Imk$, the complex group velocity $\frac{\partial\omega}{\partial k}$, etc. In the context of temporal theory, for example, the wave- guide state is unstable provided $\omega_i > 0$ for any real k and the most unstable local mode has growth rate ω_i^{max}, where the superscript denotes the maximum over all real wave numbers at fixed control parameter.

New Trends in Nonlinear Dynamics and Pattern-Forming Phenomena
Edited by P. Coullet and P. Huerre
Plenum Press, New York, 1990

The foregoing criterion defines the temporal stability of a system, but it provides no information concerning the propagative character of the local modes emanating from and excited by a localized injection of energy. To describe the space-time response to any such excitation one must evaluate the group velocity and one can, therewith, specify whether any unstable modes grow *in situ* or whether all unstable modes propagate away from the source region. Clearly, a very important characteristic of an unstable system is, from this point of view, the growth rate of any mode having a vanishing group velocity (i.e., $\frac{\partial \omega}{\partial k}|_{k_0} = 0$). The growth rate of such a mode is termed the absolute growth rate and is denoted herein by ω_{0i}. The associated real frequency and complex wave number of this mode is denoted by ω_{0r} and $k_0 = k_{0r} + ik_{0i}$. If the absolute growth rate is negative, all unstable waves propagate away from the source and the system is termed convectively unstable. Alternatively, if the absolute growth rate is positive, at least one unstable mode grows in place and the system is termed absolutely unstable. For development of the technical aspects of these linear concepts the reader is referred to Sturrock (1961), Briggs (1964), Bers (1975,1983) and Lifshitz & Pitaevskii (1981).

The onset of instability as a control parameter μ exceeds its critical value for marginal stability in a wave guide possessing reflectional symmetry ($x \rightarrow -x$) is usually of absolute type. The instability fronts emanating from any localized impulse must, in such systems, spread symmetrically relative to the source and there will usually, although not necessarily, be an unstable mode with vanishing group speed. For more general wave guides without reflectional symmetry, one expects the linear dynamics to exhibit successive transitions from a stable state to a convectively unstable state to (possibly) an absolutely unstable state as the control parameter is continuously increased. This sequence with $\omega_i^{max} \geq \omega_{0i}$ for all x is expected to be generic because there is no *a priori* reason why the value of the control parameter for onset of instability μ_c should coincide with that for incipient absolute instability μ_t. The order of transitions just described can be readily verified by reference to the linear Ginzburg-Landau model

$$\left\{ \frac{\partial}{\partial t} + U\frac{\partial}{\partial x} - \mu - (1 + ic_d)\frac{\partial^2}{\partial x^2} \right\} A = 0. \tag{1.2}$$

The condition for marginal stability is $\mu_c = 0$, the parameter range for convective instability is $\mu_c < \mu < \mu_t$, and absolute instability exists for $\mu > \mu_t = U^2/[4(1 + c_d^2)]$ (cf., Chomaz, Huerre & Redekopp - hereinafter denoted as CHR, 1987,1988). When $U = 0$ the system possesses reflectional symmetry and the values of μ_c and μ_t coincide, the instability at onset being of absolute type.

The foregoing local mode description based on the assumption of translational invariance is no longer strictly valid when the basic state varies spatially along the wave guide and the propagation space is inhomogeneous. Nevertheless, as long as the inhomogeneity of the propagation space is weak, those concepts can be applied locally and one can determine the stability properties at any position along the wave guide based solely on the state at that position. The specific requirement on the strength of the inhomogeneity in order for a "local" analysis to be valid is that the ratio of the local mode wavelength to the scale of the inhomogeneity (δ, say) must be small compared to unity, a condition which is satisfied in many spatially-developing, hydrodynamic flows.

In such cases, the local state can be defined as being stable or unstable and, if it is unstable, whether it is absolutely unstable or convectively unstable. That is, one can define local values $\omega_i^{max}(\delta x), \omega_{0i}(\delta x)$, etc. which may vary slowly along the wave guide.

Different scenarios for the spatial variation of ω_i and ω_{0i} were considered in our earlier work (CHR, 1987, 1988), both for infinite and semi-infinite wave guides. In particular, it was revealed in either case that a synchronized mode exhibiting long-range spatial coherence is destabilized whenever an interval of sufficient spatial extent having local absolute instability (i.e., $\omega_{0i}(x) > 0$) exists. Such a mode is termed a global mode because it may extend over a domain encompassing the entire region of local instability, even extensive contiguous regions where the local instability is convective (i.e., where $\omega_i(x) > 0$, but $\omega_{0i}(x) < 0$). Where the inhomogeneous character of the wave guide satisfies the necessary conditions (to be prescribed later), the propagation-space dimension admits a denumerable set of eigenmodes, the gravest of which undergoes a Hopf bifurcation to a limit cycle. As the domain of absolute instability increases, a successive number of these modes are destabilized on a linear basis. The mode with the highest growth rate presumably prevails, although nonlinear effects may dramatically alter the observed dynamics, especially at high supercritical values of the control parameter. Some features of the nonlinear behavior are discussed later. The important point, however, is that global modes possess the characteristics of oscillators. This aspect is developed further with particular emphasis given to the forced response of a global mode excited by a spatially-compact source.

Criteria for specifying the onset or destabilization of global modes and their associated frequency ω_g have been derived by CHR (1989) based on a WKB analysis of a variable-coefficient, linear, Ginzburg-Landau equation (2) with arbitrary spatial variations of $\omega_0(x)$ and $k_0(x)$. The frequency of the first unstable global mode is determined, to first order in the WKB expansion parameter, by the local absolute frequency at the saddle point x_s nearest to the real axis of the function $\omega_0(x)$ in the complex x-plane. In this way we obtain that the complex frequency of a global mode satisfies the conditions

$$\omega_{gr} \sim \omega_r(x_s) + O(\delta), \tag{1.3a}$$

$$\omega_{gi} \leq \omega_{0i}(x_s) \leq \omega_{0i}^{max} \leq \omega_{i,max}^{max}, \tag{1.3b}$$

where $\omega_{i,max}^{max}$ denotes the maximum over both x and k, and where x_s is determined from the condition

$$\left.\frac{\partial \omega_0}{\partial x}\right|_{x_s} = 0. \tag{1.3c}$$

It is clear from these conditions that the destabilization of a global mode (i.e., $\omega_{gi} > 0$) requires a finite region with $\omega_{0i}(x) > 0$; that is, a finite interval of absolute instability in the wave guide. Consistent with the specific examples considered earlier (i.e., CHR 1987), we also observe that the condition

$$\int_{x_{t_1}}^{x_{t_2}} \sqrt{\omega_{0i}(x)}\, dx \geq O(1) \tag{1.4}$$

is satisfied for the existence of amplified global modes, where $x_{t_1} < x < x_{t_2}$ defines the interval on the real axis where the local state is absolutely unstable.

The global instability concepts described above have been tested in specific, hydrodynamic flows. The most extensive studies have been performed for the two-dimensional wake behind a bluff body. Local instability characteristics were calculated by Monkewitz (1988) using a two-parameter family of velocity profiles to model the spatially-developing flow. The onset of the discrete frequency, vortex-shedding mode was shown to correlate with the existence of a pocket of absolute instability and the destabilization of the global mode occurred for a Reynolds number significantly above that for local instability. Experiments by Mathis et al. (1984), Provansal et al. (1987), and Sreenivasan et al. (1987, 1989) demonstrate clearly that the onset of vortex shedding corresponds to a super-critical Hopf bifurcation to a global mode. Numerical simulations of bluff-body flows by Jackson (1987), Hannemann & Oertel (1988), and Yang & Zebib (1989) show clearly the existence of a global mode which appears at Reynolds numbers greater than that required for local instability and local absolute instability. For a comprehensive discussion of these concepts and their application to a number of spatially-developing systems, the reader is referred to a recent review by Huerre & Monkewitz (1990).

2 THEORETICAL FOUNDATIONS

Since a countable set of global modes exist which can be ordered with respect to their growth rates, only a single mode is marginal at the threshold value of the control parameter for global instability. Also, linear global modes have a discrete frequency of oscillation which is uniform over the entire extent of spatially-varying, local stability characteristics. For this reason the study of weak nonlinearity and weak forcing of the marginal mode by means of a multiple-scale analysis can be carried out in the same way as the classical results for oscillators. A study of these effects is pursued here because of the practically important issues pertaining to the control of the local and global dynamics of spatially-varying wave-guide states. The linear and nonlinear response to a localized external forcing, the relation between the response and the position of the forcing *vis-a-vis* the location of a pocket of local absolute instability, the gain or efficiency of the forcing, etc., are some important elements of global modes deserving clarification.

For the sake of brevity, the effect of weak forcing and nonlinearity will be illustrated using the model equation

$$\frac{\partial A}{\partial t} + \mathcal{L}(\frac{\partial}{\partial x}, x; \mu)A + c(x;\mu)|A|^2 A = f(x,t), \tag{2.1}$$

for the complex amplitude function $A(x,t)$. We assume that the unforced wave-guide dynamics admits $A \rightarrow Ae^{i\theta}$ symmetry and suppose that $A(x,t)$ vanishes at the boundaries of the infinite or semi-infinite domain. $\mathcal{L}$ is a linear differential operator, μ is the control parameter, and $c(x;\mu)$ is a complex coefficient of the nonlinear term. The linear homogeneous equation admits a solution of the form

$$A_g(x,t) = \phi_g(x)e^{-i\omega_g t} \tag{2.2}$$

for the gravest mode. The frequency ω_g and modal function $\phi_g(x)$ depend on μ and there exists a critical value μ_g such that the system is globally stable for $\mu < \mu_g$. At $\mu = \mu_g$ the system is neutral and $Im\omega_g(\mu_g) = 0$. The amplitude of the linearized marginal mode is unconstrained and may evolve slowly with respect to the time scale ω_g^{-1}, which we suppose is finite.

A multiple-scale analysis is performed using the small parameter ϵ ($0 < \epsilon \ll 1$) which measures the strength of the forcing and the departure from criticality:

$$f(x,t) = \epsilon^2 F \delta(x - x_f) e^{-i\omega_f t}, \tag{2.3a}$$

$$\omega_f = \omega_g + \epsilon^2 \Omega, \tag{2.3b}$$

$$\mu = \mu_g + \epsilon^2 \Delta_\mu. \tag{2.3c}$$

A slow time scale $T = \epsilon^2 t$ is introduced in order to avoid the appearance of secular terms in the perturbation expansion

$$A(x,t) = \sum_{n=1}^{\infty} \epsilon^n A_n(x,t,T). \tag{2.4}$$

Assuming that the operator $\mathcal{L}$ is analytic in the parameter μ we may write

$$\mathcal{L}\left(\frac{\partial}{\partial x}, x; \mu\right) = \mathcal{L}_g\left(\frac{\partial}{\partial x}, x; \mu_g\right) + \epsilon^2 \Delta_\mu \mathcal{L}_\mu\left(\frac{\partial}{\partial x}, x; \mu_g\right) + O(\epsilon^4). \tag{2.5}$$

Thus, the leading order term in (2.4) is described by the equation

$$\frac{\partial A_1}{\partial t} + \mathcal{L}_g\left(\frac{\partial}{\partial x}, x; \mu_g\right) A_1 = 0, \tag{2.6}$$

with the solution

$$A_1 = \mathcal{A}(T) e^{-i\omega_g t} \phi_g(x) \tag{2.7}$$

defining the neutral global mode with arbitrary amplitude $\mathcal{A}(T)$. The next order term A_2 satisfies the same homogeneous equation as (2.6) and provides no essential information or constraint concerning $\mathcal{A}(T)$. A compatibility condition for the avoidance of secular terms at third order leads to the following evolution equation for the global mode amplitude:

$$\frac{d\mathcal{A}}{dT} = \Delta_\mu \frac{<\psi|\mathcal{L}_\mu \phi_g>}{<\psi|\phi_g>} \mathcal{A} - \frac{<\psi|c(x;\mu)|\phi_g|^2 \phi_g>}{<\psi|\phi_g>} |\mathcal{A}|^2 \mathcal{A} - F \frac{\psi^*(x_f)}{<\psi|\phi_g>} e^{-i\Omega T}. \tag{2.8}$$

The quantity $< f|g >$ denotes the scalar product $\int f^* g \, dx$, superscript * denotes the complex conjugate, and $\psi(x)$ is the solution of the equation

$$\left\{ i\omega_g^* + \mathcal{L}_g^A\left(\frac{\partial}{\partial x}, x; \mu_g\right) \right\} \psi = 0, \tag{2.9}$$

where $\mathcal{L}_g^A$ is the adjoint of $\mathcal{L}_g$.

The result (2.8) could be anticipated from the well-established results for weakly nonlinear oscillators. We emphasize here, however, that the dynamical state of the entire wave guide behaves like a single oscillator with a coherent spatial structure. When the forcing amplitude F vanishes, $\mathcal{A}(T)$ evolves according to the familiar Landau equation. When $F = O(1)$ an imperfect bifurcation occurs with the familiar result that an $O(\epsilon^2)$ forcing can generate an $O(\epsilon)$ response, even when the basic state is linearly

damped (i.e., $\Delta_\mu < 0$). The forcing efficiency and phase shift of the response are determined by $\psi^*(x_f)$.

In order to exhibit explicit results for the forcing and to determine the sub- or super-critical nature of the bifurcation, we take a specific form for the operator $\mathcal{L}$. The form chosen is that of the Ginzburg-Landau equation with

$$\mathcal{L}\left(\frac{\partial}{\partial x}, x; \mu\right) = -\left\{p(x;\mu) - U\frac{\partial}{\partial x} + b\frac{\partial^2}{\partial x^2}\right\}. \tag{2.10}$$

where U is a constant, real advection velocity and b is a complex constant related to the curvature of the local dispersion relation for the wave guide. The adjoint operator is

$$\mathcal{L}^A\left(\frac{\partial}{\partial x}, x; \mu\right) = -\left\{p^*(x;\mu) + U\frac{\partial}{\partial x} + b^*\frac{\partial^2}{\partial x^2}\right\}. \tag{2.11}$$

The important difference between $\mathcal{L}$ and its adjoint is in the sign of the advection term which has been reversed in the two operators. A convenient choice for the term $p(x;\mu)$ for an infinite wave guide is

$$p(x;\mu) = \mu_0 + \frac{1}{2}\mu_2(x - z_0)^2 + \epsilon^2\Delta_\mu, \tag{2.12}$$

in which μ_0 is real and μ_2 and z_0 are complex constants. With this choice the solution for the global modes has

$$\omega_{g_n} = i\mu_0 - \frac{i}{4}\frac{U^2}{|b|}e^{-i\theta_b} - i(2n+1)\left|\frac{\mu_2 b}{2}\right|^{1/2} e^{i(\theta_{-\mu_2}+\theta_b)/2} \tag{2.13a}$$

$$\phi_{g_n}(x) = \exp\left\{\frac{1}{2}\frac{U}{b}x - \frac{1}{2}\left|\frac{\mu_2}{2b}\right|^{1/2}(x - z_0)^2 e^{i(\theta_{-\mu_2}+\theta_b)/2}\right\}\cdot H_n\left(\left|\frac{\mu_2}{2b}\right|^{1/4}(x - z_0)e^{i(\theta_{-\mu_2}+\theta_b)/4}\right), \tag{2.13b}$$

where $H_n(x)$ are the Hermite polynomials of order n, $\theta_{-\mu_2} = \arg(-\mu_2)$, and $\theta_b = \arg(b)$. The adjoint function is given by

$$\psi_n(x) = \exp\{-Ux/b^*\}\phi^*_{g_n}(x). \tag{2.14}$$

The reversed effect of advection in the adjoint is clearly evident and, by reference to (2.8), its role in regard to forcing efficiency is to shift the optimal location of forcing considerably upstream of the maximum signature of the global mode. This is demonstrated clearly in numerical simulations presented in the next section.

In order for the global mode to be marginal (i.e., $Im\omega_{g_n} = 0$), the control parameter μ_0 must take the value

$$\mu_0 \equiv \mu_{g_c} = \frac{1}{4}\frac{U^2}{|b|}\cos\theta_b + (2n+1)\left|\frac{\mu_2 b}{2}\right|\cos\left(\frac{\theta_{-\mu_2}+\theta_b}{2}\right). \tag{2.15}$$

Restricting attention to the first mode to be destabilized (i.e., $n = 0$), the Landau constant (i.e., the coefficient of the nonlinear term in (2.8)) can be evaluated analytically for specific choices of the coefficient $c(x;\mu_g)$ multiplying the nonlinear term in (2.1). We adopt the simple choice $c(x;\mu_g) = 1 + ic_n$ where c_n is a real constant in all that follows. For these conditions we obtain the following results:

$$< \psi_0 | \phi_{g_0} >= \int_{-\infty}^{\infty} \psi_0^* \phi_g dx = \left| \frac{2b\pi^2}{\mu_2} \right|^{1/4} e^{-i\Theta/2}; \tag{2.16}$$

$$\begin{aligned} \ell &= \frac{< \psi_0 | c(x;\mu_g) |\phi_{g_0}|^2 \phi_{g_0} >}{< \psi_0 | \phi_{g_0} >} \\ &= \frac{1 + ic_n}{[3\cos^2\Theta + 1]^{1/4}} \exp \left\{ \frac{\frac{U^2}{|b|^2}\cos^2\theta_b + 6\left|\frac{\mu_2 z_0^2}{b}\right| \sin^2\theta_{z_0}}{4\left|\frac{\mu_2}{2b}\right|^{1/2}(3\cos^2\Theta + 1)}(2\cos\Theta - i\sin\Theta) \right. \\ &+ \frac{U|z_0/b|\cos\theta_b}{3\cos^2\Theta + 1}\left[\frac{5}{2}\cos\theta_{z_0} + \frac{3}{2}\cos(2\Theta + \theta_{z_0}) + 2i\sin\theta_{z_0}\right] \\ &\left. -\frac{i}{2}\tan^{-1}\left(\frac{\sin\Theta}{2\cos\Theta}\right) + \frac{i\Theta}{2} \right\}, \end{aligned} \tag{2.17}$$

where

$$\Theta = \frac{1}{2}(\theta_{-\mu_2} - \theta_b), \quad \theta_{z_0} = \arg(z_0). \tag{2.18}$$

There is no apparent information to be gleaned from this expression aside from the fact that the Landau constant for the local bifurcation bears no specific relation to that for the global bifurcation. Furthermore, even though the local bifurcation in this instance is supercritical, the global bifurcation may be either subcritical or supercritical.

3 NUMERICAL EXPERIMENTS

3.1 Nonlinear effects in free global modes

Numerical simulations of the nonlinear equation (2.1) with $\mathcal{L}$ defined by (2.10), $b = 1+ic_d$, and $c(x;\mu) = 1+ic_n$, where c_d and c_n are real constants, have been performed for two different wave-guide configurations. One configuration had the quadratic variation of $p(x;\mu)$ given in (2.12) (with μ_0, μ_2 real and $z_0 = \Delta_\mu = 0$) on an infinite domain. In this case the local wave-guide state is stable at $x = \pm\infty$ and a single region of absolute instability, bordered by symmetric regions of convective instability, exists in the vicinity of the origin. The spatial extent of the region of local absolute instability is controlled by the parameter μ_0 for fixed μ_2. The other configuration had a semi-infinite domain $0 < x < \infty$ with a linear variation of $p(x;\mu)$ having negative slope

$$p(x;\mu) = \mu_0 + \mu_1 x, \quad Re\mu_1 < 0, \; Im\mu_1 = 0. \tag{3.1}$$

A homogeneous boundary condition was imposed at $x = 0$ where the local state is absolutely unstable for sufficiently large values of μ_0 (i.e., $\mu_0 > \mu_t = U^2/[4(1 + c_d^2)]$). This region is followed by an interval of convective instability and then a region which is stable as x tends to infinity. These two configurations are simple examples of spatially-inhomogeneous wave guides possessing a single interval of absolute instability whose length is related to the control parameter μ_0.

The finite-difference code used in the present simulations was identical to that employed in our earlier studies (CHR 1987, 1988). It was demonstrated in that work that

the analytically-derived linear eigenfunction was indeed the first mode to be destabilized. The predicted values of the threshold control parameter and the eigenfrequency were also verified in the limit as the spatial and temporal discretization were reduced (a one percent error for $\Delta x = 0.5$, $\Delta t = 7.5 \times 10^{-3}$ and a 0.3 percent error for $\Delta x = 0.25$, $\Delta t = 2.0 \times 10^{-3}$). The new results to be presented here were obtained using the following set of parameters: $U = 6$, $c_d = -10$, $\mu_1 = -1.19 \times 10^{-4}, \mu_2 = -2.534 \times 10^{-6}$, $\Delta x = 0.5$, $\Delta t = 7.5 \times 10^{-3}$. The value of c_n is taken to be zero except in cases where noted otherwise. The choice of parameters, particularly for U and c_d, was made in order to compare our results with those of Deissler (1985,1987) for a constant-coefficient, convectively unstable case.

The structure of the bifurcation to the lowest-order global mode is revealed in Figures 1 and 2. Figure 1 pertains to the quadratic form for $p(x;\mu)$ on the infinite domain and Figure 2 pertains to the linear form for $p(x;\mu)$ on the semi-infinite domain. Both figures exhibit the same feature; namely, a linear variation with slope unity of the initial growth rate with respect to μ_0/μ_t, where μ_t defines the value of the control parameter for the onset of local absolute instability at $x = 0$. The figures also show the equilibrium, finite amplitude $\bar{A}$ of the global mode by plotting the maximum of the saturated state as a function of the supercriticality. It is difficult to obtain results for very small supercriticality because the time to approach equilibrium tends to infinity as $\mu_0 - \mu_{g_c}$ tends to zero. For example, 1.2×10^6 time steps were required to arrive at a good

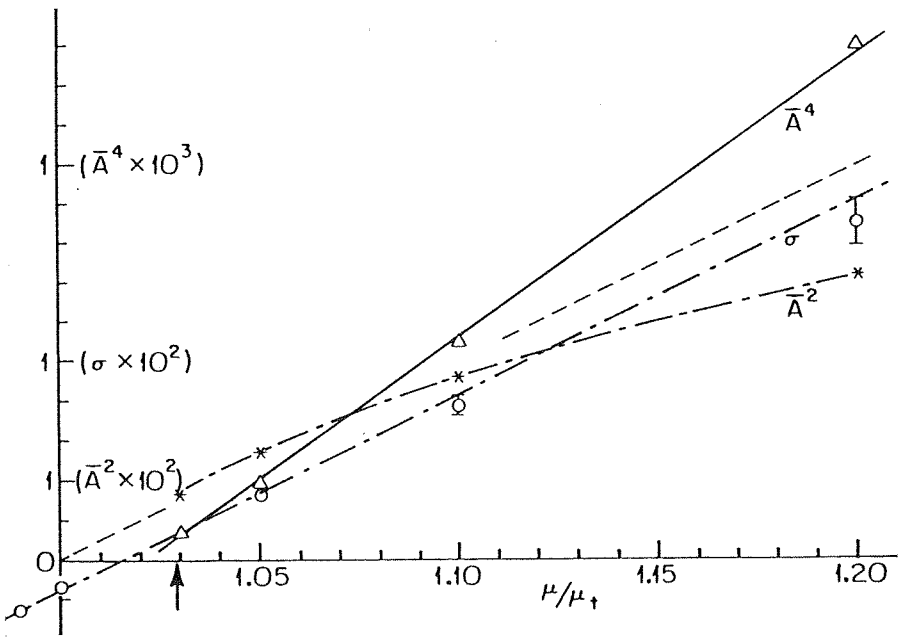

Figure 1 The bifurcation diagram for global modes in an infinite domain with a single interval of quadratically-varying absolute growth rate: – o – measured growth rate σ; – $*$ – variation of the square $\bar{A}^2$ of the peak saturation amplitude; – $\triangle$ – variation of the quartic $\bar{A}^4$ of the peak saturation amplitude. The dashed line has unit slope for σ vs. μ/μ_t. The vertical arrow denotes the theoretical bifurcation value μ_{g_c}/μ_t.

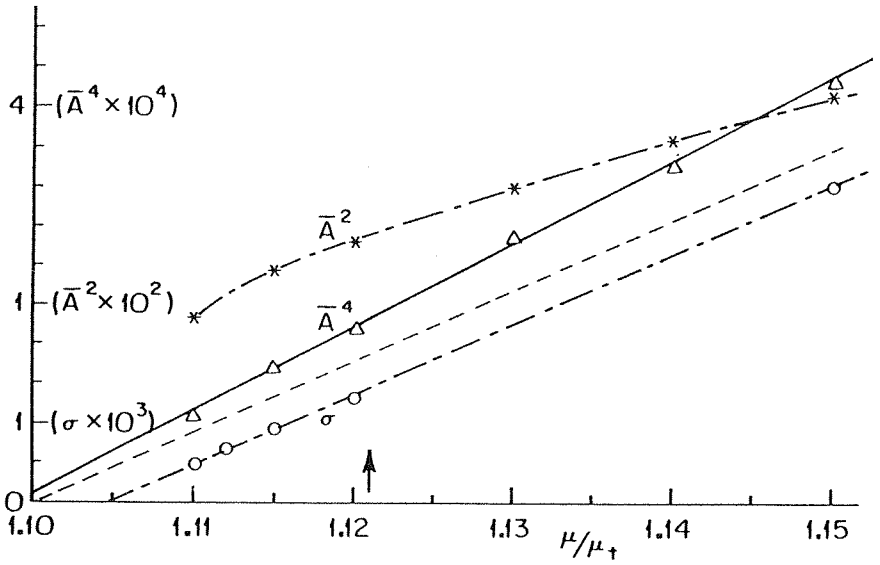

Figure 2 The same diagram as Fig. 1 for global modes in a semi-infinite domain with a single interval of linearly-varying absolute growth rate adjacent of the left boundary of the spatial domain.

estimate of the equilibrium amplitude at the smallest condition shown in Figure 2. On each figure we show variations of both quadratic and quartic values of the amplitude as well as the theoretically-derived value for the bifurcation parameter in an attempt to clarify the scaling law for the bifurcation. Using the specified numerical values of the parameters in equation (2.17), the Landau constant is $\ell = 1.1245 - 0.0526i$, suggesting that the bifurcation is supercritical. It is clear that either of three possibilities must exist: i) the values of $\mu_0 - \mu_{g_c}$ are too large to reveal the true scaling near the bifurcation point; ii) the next nonlinear term (i.e., $|\mathcal{A}|^4\mathcal{A}$) in the amplitude expansion dominates over the $|\mathcal{A}|^2\mathcal{A}$ term ; or iii), the true nonlinear evolution exhibits a subcritical bifurcation. For both wave-guide configurations, the data for $\bar{A}^4$ lie on a straight line which crosses the abscissa close to the point where the computed growth rate vanishes. This is strongly suggestive that the higher order nonlinear term dominates the equilibrium state. Of course, more simulations are needed to clarify the issue.

The theoretical development in the previous section deals exclusively with the global mode dynamics in the immediate vicinity of critical. It predicts the shape of the global mode very well for $|\mu_0 - \mu_{g_c}|/\mu_{g_c} \ll 1$, but the theory gives no indication as to how the mode characteristics change for finite values of the supercriticality. This issue was investigated and sample results are shown in Figure 3 for the infinite wave-guide configuration. It is evident that the maximum of the global mode moves upstream and the mode shape broadens as the supercriticality increases. The left column depicts the envelope of the mode with the advective factor $\exp(Ux/2b)$ subtracted (i.e., the nonlinear extension of the function $\phi_g(x)$ in (2.13b) with $U = 0$). One observes that this "transformed" mode is virtually unchanged in shape, but its maximum is shifted upstream as the nonlinearity increases. One interpretation of this effect is that it is due to the "mean flow" contribution to the growth rate (i.e., considering the combined effect of the terms $p(x;\mu) - (1 + ic_n)|A|^2$ as an effective growth rate). Based on this

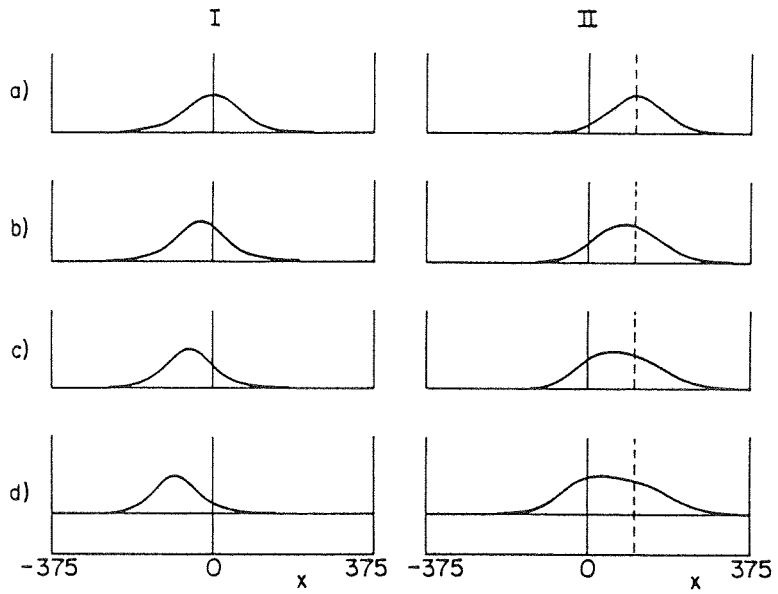

Figure 3 Nonlinear states for global modes in an infinite domain. The left column shows the modulus of the "transformed" global mode $|\phi_g(x)\exp(-Ux/2b)|$ and the right column shows the modulus of the global mode $|\phi_g(x)|$. a) The linear global mode. b) The nonlinear global mode for a supercriticality $(\mu_0 - \mu_{g_c})/\mu_{g_c} = 0.024$. c) Same as b) for a supercriticality of 0.073. d) Same as b) for a supercriticality of 0.171. The vertical line marks the location of the peak absolute growth rate and the dashed line marks the peak of the linear global mode.

point of view, the nonlinear effect shifts the position of the absolute instability and, therewith, the position of the global mode.

As indicated above, most of our numerical experiments were performed with $c_n = 0$ and, consequently, $1 + c_d c_n > 0$. In this case the uniform Stokes wave-train solutions of the constant-coefficient, Ginzburg-Landau equation are linearly stable with respect to the Benjamin-Feir mechanism (cf., Newell, 1974). The global modes are stable even for strong nonlinearity under these conditions. However, the criterion $1 + c_d c_n > 0$ is only a necessary condition for the stability of global modes. This is why a stable global mode was found for a numerical simulation with $c_n = 1$ $(1 + c_d c_n = -9)$ and a supercriticality $(\mu_0 - \mu_{g_c})/\mu_{g_c}$ of 43% (see Figure 4a). On the contrary, when $c_n = 10$ and all other parameters are unchanged, a very irregular state is observed (cf., Figure 4b). Furthermore, the irregular state persists even when the supercriticality is small. Figure 5 presents, for $(\mu_0 - \mu_{g_c})/\mu_{g_c} = 0.07$, the saturated regular mode for $c_n = 0$ and the corresponding irregular mode when $c_n = 10$. In both sets of figures the global mode for $c_n = 10$ exhibits a regular spatial structure and a complex time behavior over the initial regions in x. This early region is followed by a pulse-like structure with a fairly regular spatial periodicity.

The chaotic-type global mode for large negative values of $1 + c_d c_n$ merits a much more comprehensive study. The present exploratory simulations reveal a little of the

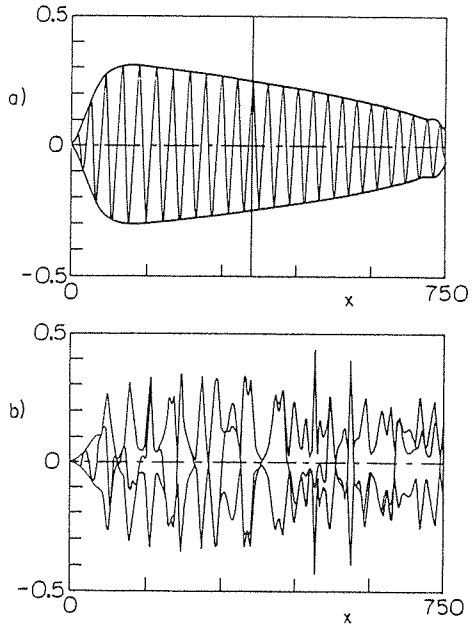

Figure 4 The envelope and the real part of the nonlinear global mode in a semi-infinite domain obtained for a supercriticality $(\mu_0 - \mu_{g_c})/\mu_{g_c} = 0.43$. a) $c_n = 1$. b) $c_n = 10$. The vertical line in a) marks the end of the absolutely unstable region and both structures are obtained at the same time $(3 \times 10^5 \Delta t)$.

variety of free, dynamical states possible in spatially-varying wave guides and their connection to regions of local absolute instability.

3.2 Forced response of global modes

The parameter space to be considered in a study on the effect of forcing is quite large since the strength, frequency, and position of forcing are added to those characterizing the homogeneous problem. For this reason the present results are limited to exploring the influence of the forcing location x_f (*vis-a-vis* the absolutely unstable region) and the shape of the response, which is predicted to be close to the free, linear global mode when the forcing is weak and the wave-guide state is close to critical.

The important elements in the forced response of the lowest (i.e., $n = 0$) linear, marginal mode for the infinite-domain configuration (see Eqn. 2.13 - 14) are shown in Figure 6 for the same set of parameters used in the earlier simulations; $U = 6$, $c_d = -10$, and $\mu_2 = -2.534 \times 10^{-6}$. The free mode, whose envelope is a simple Gaussian when $n = 0$, is shown in Figure 6a in its position relative to the maximum absolute growth rate denoted by the vertical line in the figure. The strongest action of the global mode is found downstream of the absolutely unstable region. When the factor $\exp(Ux/2b)$ is

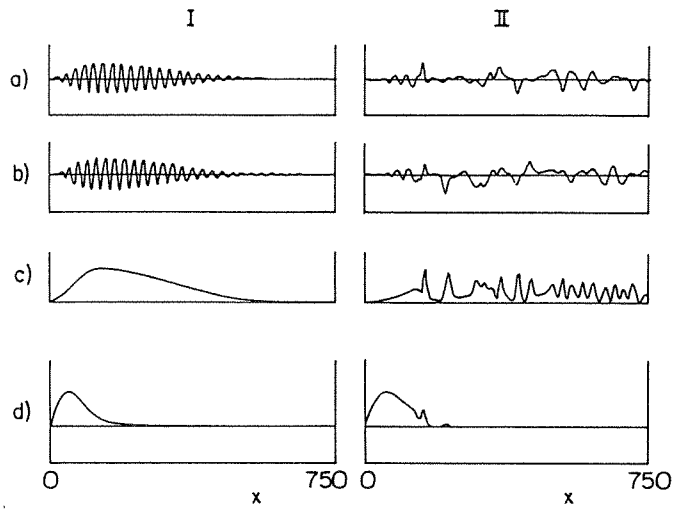

Figure 5 The nonlinear global mode in a semi-infinite domain obtained for a supercriticality of 0.07. The left column is for $c_n = 0$ and the right column is for $c_n = 10$. a) The real part of $\phi_g(x)$. b) The imaginary part of $\phi_g(x)$. c) The modulus of $\phi_g(x)$. d) The modulus of $\phi_g(x)\exp(-Ux/2b)$.

removed from the eigenfunction (cf., Eqn. 2.13b), the remainder is a Gaussian centered over the region of absolute instability as seen in Figure 6b. The relationship to the forcing efficiency is revealed in Figure 6c where the envelope of the adjoint function (2.14) is included. The adjoint is shifted upstream from the peak absolute growth rate by an amount ($\delta x = 112.5$) equal to the downstream shift of the global mode.

The important result just described regarding the forcing efficiency was tested in numerical simulations of the nonlinear equation with $c_n = 0$ and with $\epsilon^2\Delta_\mu = -0.027\mu_t$, $\epsilon^2 F = 10^{-5}$, $\epsilon^2\Omega = 0.006$. The neutral values for the free global mode are $\mu_0 = 1.017\mu_t$ and $\omega_g = 0.884$. The forced response is shown in Figure 7 as the forcing location is varied from upstream to downstream of the peak of the adjoint function which is located at $x = -112.5$. Figure 7a shows the free mode shape for this (weakly) nonlinear realization and it corresponds very closely to the linear mode. Since the simulation is performed for a slightly subcritical setting of the control parameter, this mode would ultimately decay. In the remaining panels of the figure, however, a finite equilibrium amplitude is sustained by virtue of the forcing which is most effective when it is positioned at or slightly downstream of the peak of the adjoint function. The forced response is observed to move upstream as the forcing is displaced downstream of its optimum location, but the response does not follow the theoretical prediction in that the equilibrium amplitude does not scale directly with $\psi^*(x_f)$ which is symmetric about $x = -112.5$. It is worth noting that the response reaches an amplitude which is several orders of

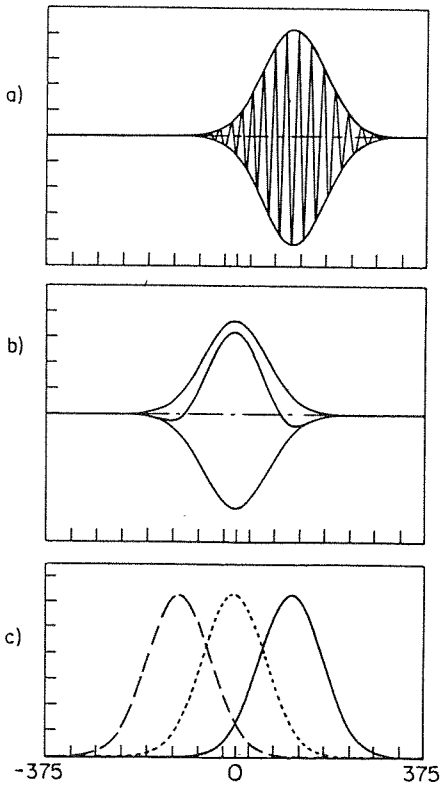

Figure 6 The linear, free global mode in the infinite domain. a) The modulus and real part of $\phi_g(x)$. b) The modulus and real part of the "transformed" mode $\phi_g(x)\exp(-Ux/2b)$. c) — $|\phi_g(x)|$; - - - - $|\phi_g(x)\exp(-Ux/2b)|$; - - - $|\psi_0(x)|$.

magnitude larger than the forcing, a result in agreement with predictions of weakly nonlinear theory. The numerical simulations for the last two cases shown in Figure 7 revealed an important nonlinear effect in that there was a distinct temporal oscillation of the forced response. This dynamical state having temporal quasi-periodicity with a coherent spatial structure is interesting and deserves further investigation. It may explain the observed departures from predictions based on weakly nonlinear theory as noted above and exhibited in more detail in Figure 8. Figure 8 shows two different measures of the forcing efficiency for the same set of experiments. One is simply the global maximum of the response and the other is the square-root of the total energy of the response. Both measures show that the peak efficiency occurs for forcing locations upstream of the maximum absolute growth rate, but downstream of the position suggested by linear theory. The discrepancies must derive from nonlinear effects.

4 CONCLUDING REMARKS

The results presented here, reveal important characteristics of global modes. The necessary condition of an interval of local absolute instability for the existence of a global

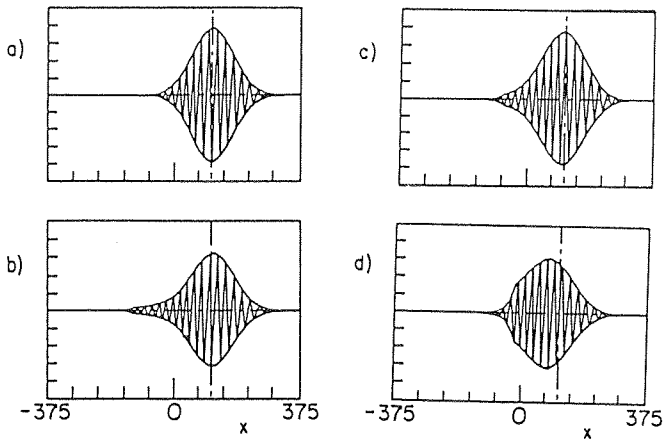

Figure 7 The forced, nonlinear response for a weakly-damped global mode in the infinite domain. a) The linear eigenfunction. b) The response with forcing at $x_f = -125$; the peak response amplitude is $\bar{A} = 2.5 \times 10^{-3}$. c) Same as b) with $x_f = -75$, $\bar{A} = (4.4 \pm 0.5) \times 10^{-3}$. d) Same as b) with $x_f = -25$, $\bar{A} = 2.5 \times 10^{-3}$.

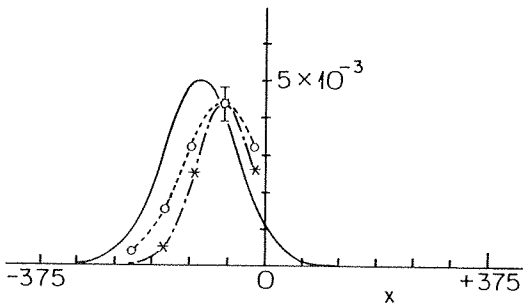

Figure 8 The forcing efficiency for the same parameters used in the simulations shown in Figure 7. — the linear, theorectical prediction; - - o - - the maximum response amplitude; – * – the square root of the total response energy.

mode, and the significance of these modes in the dynamics of spatially-inhomogeneous wave guides, is firmly established. However, there exists a rich and diverse spectrum of nonlinear effects which await careful study, even in the context of the simplified models discussed herein.

It is clear from the present work that the specific details and location of the absolutely unstable region do not necessarily determine the location of the "action" of global modes. Their "action" is felt in regions well beyond that where the local state is absolutely unstable and the most efficient location to force such modes also lies outside (and considerably upstream) of the region of absolute instability. In parameter domains where these modes are stable, they impose a long-range order to the wave guide and are responsible for the existence of discrete frequencies which are quite unrelated to those frequencies associated with the local state. The present work also shows that the effect of nonlinearity and forcing on these modes open the possibility of frequency and mode competition which can lead to a host of complex spatio-temporal dynamical states. Studies based on models and of spatially-developing wave guides in applications remain a fruitful area of study.

ACKNOWLEDGEMENTS

This work was supported by the U.S. Air Force Office of Scientific Research under Contract No. F49620-85-C-0080.

REFERENCES

1. Bers, A., 1975. Linear waves and instabilities. *Physique de Plasmas*, eds. C. DeWitt and J. Peyraud, pp. 117-215. Gordon and Breach, New York.

2. Bers, A., 1983. Space-time evolution of plasma instabilities-absolute and convective. *Handbook of Plasma Physics*, eds. M.N. Rosenbluth and R.Z. Sagdeev, pp. 1: 451-517. North-Holland, Amsterdam.

3. Briggs, R. J., 1964. *Electron-Stream Interaction with Plasmas.* MIT Press, Cambridge.

4. Chomaz, J. M., Huerre, P., and Redekopp, L. G., 1987. Models of hydrodynamic resonances in separated shear flows. Proc. 6th Symp. Turb. Shear Flows, pp. 3.2.1-6.

5. Chomaz, J. M., Huerre, P., and Redekopp, L. G., 1988. Bifurcations to local and global modes in spatially-developing flows. *Phys. Rev. Lett.*, 60: 25-28.

6. Chomaz, J. M., Huerre, P., and Redekopp, L. G., 1989. A frequency selection criterion in spatially-developing flows. *Stud. Appl. Math.*, (submitted for publication).

7. Deissler, R. J., 1985. Noise-sustained structure, intermittency, and the Ginzburg-Landau equation. *J. Stat. Phys.*, 40: 371-95

8. Deissler, R. J., 1987. Spatially-growing waves, intermittency and convective chaos in an open-flow system. *Physica D*, 25: 233-260

9. Hannemann, K., and Oertel, Jr. H., 1988. Numerical simulation of the absolutely and convectively unstable wake. *J. Fluid Mech.*, 199: 55-88.

10. Huerre, P., and Monkewitz, P. A., 1990. Local and global instabilities in spatially-developing flows. *Ann. Rev. Fluid Mech.*, Vol. 22 (in press).

11. Jackson, C. P., 1987. A finite-element study of the onset of vortex shedding in flow past variously shaped bodies. *J. Fluid Mech.*, 182: 23-45.

12. Lifshitz, E. M., and Pitaevskii, L. P., 1981. *Physical Kinetics.* Chapter VI. Pergamon, London.

13. Mathis, C., Provansal, M., and Boyer, L., 1984. The Bénard-von Karman instability: an experimental study near the threshold. *J. Phys. Lett.* (Paris), 45: 483-491.

14. Monkewitz, P. A., 1988. The absolute and convective nature of instability in two-dimensional wakes at low Reynolds numbers. *Phys. Fluids*, 31: 999-1006.

15. Newell, A. C., 1974. Envelope equations. *Lect. Appl. Math.*, ed A.C. Newell, Vol. 15, pp. 157-163. *Am. Math. Soc.*, Providence, RI.

16. Provansal, M., Mathis, C., and Boyer, L., 1987. Bénard-von Karman instability: transient and forced regimes. *J. Fluid Mech.*, 182: 1-22.

17. Sreenivasan, K. R., Strykowski, P. J., and Olinger, D. J., 1987. Hopf bifurcation, Landaw equation and vortex shedding behind circular cylinders. *Proc. Forum on Unsteady Flow Separation*, ed. K. N. Ghia. ASME FED. Vol. 52.

18. Sreenivasan, K. R., Strykowski, P. J., and Olinger, D. J., 1989. On the Hopf bifurcation and Landau-Stuart constants associated with vortex 'shedding' behind circular cylinders. *J. Fluid Mech.*, (submitted for publication).

19. Sturrock, P. A., 1961. Amplifying and evanescent waves, convective and non-convective instabilities. *Plasma Physics*, ed. J.E. Drummond, pp. 124-42. McGraw-Hill, New York.

20. Yang, X. and Zebib, A., 1989. Absolute and convective instability of a cylinder wake. *Phys. Fluids*, A1: 689-696.